Model Evaluation

The new backflow model was included as a module in the $k-L$ and $k-\epsilon$ turbulence models available in the USA Reynolds-averaged Navier-Stokes solver.[4] Several flow cases were computed and the results agreed well with experimental data. Two of these cases are presented here:

Case 1

This case is the transonic flow over an axisymmetric bump of Bachalo and Johnson.[5] Figure 2 presents comparisons between predictions and data for surface pressure, skin friction, axial velocity profiles at two streamwise locations within the reversed flow region, and the corresponding Reynolds shear stress and turbulence kinetic energy profiles. Pressure contours are also included to show the shock location. The host turbulence model was the one-equation $k-L$ model.[1] For comparison, the figure includes computation results without incorporation of the backflow module.

It is seen that k_{max} is underpredicted by about 50%; however, since Eq. (8) involves $k_{max}^{1/2}$, this translates into a 29% underprediction of the eddy-viscosity magnitude, not severe enough to harm the overall predictive quality, especially that of the wall pressure distribution. It is also noted that the skin-friction prediction is inferior to that shown in Ref. 1, using the algebraic backflow model. However, the current model is based on a more rigorous derivation that avoids the need for a near-wall term as in the old model. Therefore, the new model deserves further evaluation before a fair comparison of the two models is possible.

Case 2

This case is the hypersonic axisymmetric flow over an ogive-cone-cylinder 35-deg flare configuration of Kussoy and Horstman.[6] Figure 3 shows predictions and data comparisons for surface pressure, skin friction, and surface heat transfer. The pressure contour plot is included to show shock structure and extent of upstream influence. Here, too, the $k-L$ turbulence model served as the host model.

Summary

A model for turbulent backflows was introduced and tested. The model is based on experimental observations, in particular, the wake-like behavior of the turbulence and the type of energy balance observed in detached flow regions. This leads to an ODE for the eddy viscosity, resulting from a reduced form of the kinetic energy equation. This ODE is solvable analytically. The model is applied as a module within a "host" eddy-viscosity model (such as a $k-\epsilon$ model) to predict the eddy-viscosity field inside backflow regions. Predictions of several reversed flow cases are encouraging. Further testing of this model, covering a wide range of Mach numbers and geometries, will be reported in future work.

References

[1]Goldberg, U. C., and Chakravarthy, S. R., "Separated Flow Predictions Using a Hybrid $k-L$/Backflow Model," *AIAA Journal*, Vol. 28, No. 6, 1990, pp. 1005–1009.

[2]Simpson, R. L., "A Review of Some Phenomena in Turbulent Flow Separation," *Transactions of ASME, Journal of Fluids Engineering*, Vol. 103, Dec. 1981, pp. 520–533.

[3]Delery, J. M., "Experimental Investigation of Turbulence Properties in Transonic Shock/Boundary-Layer Interactions," *AIAA Journal*, Vol. 21, No. 2, 1983, pp. 180–185.

[4]Chakravarthy, S. R, Szema, K.-Y., and Haney, J. W., "Unified 'Nose-to-Tail' Computational Method for Hypersonic Vehicle Applications," AIAA Paper 88-2564, Williamsburg, VA, June 1988.

[5]Bachalo, W. D., and Johnson, D. A., "An Investigation of Transonic Turbulent Boundary Layer Separation Generated on an Axisymmetric Flow Model," AIAA Paper 79-1479, 1979.

[6]Kussoy, M. I., and Horstman, C. C., "Documentation of Two- and Three-Dimensional Hypersonic Shock Wave/Turbulent Boundary Layer Interaction Flows," NASA TM 101075, Jan. 1989.

Effect of Leading-Edge Geometry on a Turbulent Separation Bubble

N. Djilali*
University of Victoria, V8W 3P6 Canada
and
I. S. Gartshore†
University of British Columbia, Vancouver, V6T 1W5 Canada

Introduction

SEPARATION bubbles are found in a variety of fluid dynamics devices and processes, and they often have a critical impact on performance. Understanding of the mechanisms which affect and control the size and characteristics of separation bubbles is therefore important. Several studies on sharp-edged bluff bodies[1-3] have shown that increased freestream turbulence can reduce the separation bubble size by up to 45%. The shortening of the bubble is attributed to an increased spreading rate of the separated shear layer, but there is yet no comprehensive explanation for the interaction mechanism between the stream turbulence and the separated shear layer. Dziomba[4] used trip wires on the front face of a blunt rectangular plate to control the separation bubble length. The trip wire was found to have the same qualitative effect as an increase in freestream turbulence; however, it was argued that the shortening of the bubble was mostly due to an alteration of the front face geometry resulting in an effective change in the angle of separation.

This Note presents the results of an experimental study showing the effect of the separation angle on both pressure distribution and size of a separation bubble forming on a blunt thick plate (Fig. 1). Flow-visualization results for laminar and transitional flow on a similar geometry were reported by Ota et al.[5] The present measurements were made at a fully turbulent, Reynolds-number-independent flow regime ($Re = 5 \times 10^4$), and the reattachment lengths were deduced directly from surface measurements using a pulsed-wire wall probe.

Model and Experimental Facility

The experiments were conducted in the $2.4 \times 1.6 \times 25$ m University of British Columbia (UBC) low-speed wind tunnel. A model that was previously used for detailed measurements of the turbulent flowfield around a blunt rectangular plate[6] was modified for the present experiments. The model had a chord of 800 mm, a thickness D of 89.9 mm (3.5 in.)—corresponding to a solid blockage ratio BR of 5.6%—and a span between end plates of 1000 mm, giving an aspect ratio AR of 11.1. The angle α at which the shear layer separates from the plate could be altered (from 45–90 deg) by attaching various triangular front pieces to the modified front face of the model.

Two-dimensionality and symmetry (spanwise and top-to-bottom) were verified by surface flow visualization and mean pressure measurements. The use of side plates and side extensions ensured a nominally two-dimensional separation region extending over the central two-thirds portion of the plate. The surface pressure distribution was measured using a Barocel differential pressure transducer and a 48-port Scanivalve system connected to a series of pressure taps along the centerline of the model. The mean reattachment length x_r, defined as the

Received April 11, 1991; revision received June 7, 1991; accepted for publication June 13, 1991.

*Assistant Professor, Department of Mechanical Engineering. Member AIAA.

†Professor, Department of Mechanical Engineering.

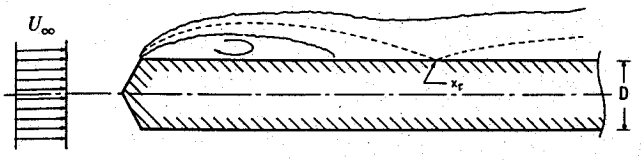

Fig. 1 Schematic of flow on a blunt thick plate.

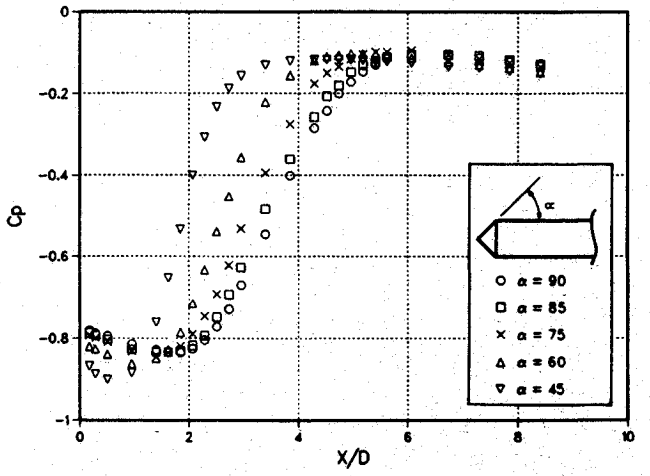

Fig. 2 Effect of separation angle on surface pressure distribution.

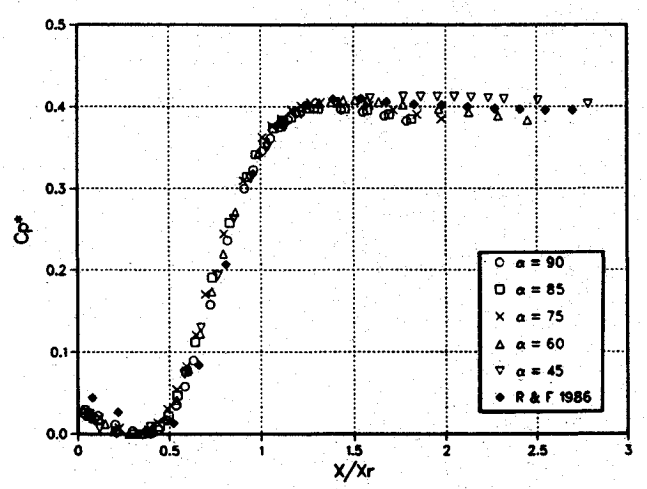

Fig. 3 Reduced pressure distributions of Fig. 2 and comparison with flat-plate/splitter-plate data of Ruderich and Fernholz.[9]

location where the mean wall shear stress vanishes, corresponds also[6] to the location where the forward-flow fraction γ is equal to 0.50; this characteristic was used to deduce x_r directly from the forward-flow-fraction measurements. These were obtained using a pulsed-wire wall probe[7] which was mounted on a sliding block, flush with the surface of the model.

Results and Discussion

The angle α at which the shear layer separates from the front face of the blunt plate has a significant impact on the pressure distribution, as shown in Fig. 2. All curves exhibit a similar behavior, with a small initial dip in the pressure coefficient $[C_P = (p-p_\infty)/(0.5\rho U_\infty^2)]$, followed by a region of approximately constant pressure, and then a rapid recovery. Decreasing the separation angle induces an earlier pressure recovery and a shift of the pressure distributions towards the leading edge with a corresponding shortening of the separation bubble length. The base presure coefficient C_{P_b}, measured at $X/D = 0.17$ (location of first pressure tap), decreases and the pressure dip immediately downstream of separation becomes more pronounced.

It is well known that separated reattaching flows have very similar pressure distributions, and that a reasonable collapse of the data is obtained over a wide range of geometries when the pressure is plotted, as suggested by Roshko and Lau,[8] in terms of x/x_r and the reduced pressure coefficient

$$C_{p^*} = \frac{C_p - C_{p\min}}{1 - C_{p\min}} \tag{1}$$

Using these reduced coordinates, the pressure distributions of Fig. 2 are replotted in Fig. 3. Data obtained from another reattaching flow, the flat-plate/splitter-plate geometry,[9] is also included for comparison. The collapse of the data onto a single curve, with slight deviations of the flat-plate/splitter-plate data, is quite remarkable and confirms that the reattachment length x_r is a basic length scale for separated reattaching flows.

The recovery pressure rise coefficient $C_{P_m^*}$, which measures the difference between the highest and lowest pressures, was found to be equal to 0.4 as compared to an averaged value of 0.36 from a variety of configurations.[8] Tani (quoted in Ref. 10) noted that the ultimate pressure recovery is higher for thinner boundary layers at separation. This is consistent with the present results since the effective thickness of the boundary layer is, here, quite small as a result of the strongly favorable pressure gradients at separation.

The variation with separation angle of C_{P_b} and x_r (measured using the wall probe) are shown in Fig. 4. The reattachment length for $\alpha = 45$ deg is about 50% shorter than for the base model ($\alpha = 90$ deg) while C_{P_b} is about 10% lower due to the lower radius of curvature of the separating shear layer. Noting a similar behavior of x_r vs α for the forebody/splitter-plate geometry, Simpson[11] proposed a correlation of the form $[x_r(\alpha) - x_r(0 \text{ deg})]/[x_r(90 \text{ deg}) - x_r(0 \text{ deg})] = \sin\ \alpha$, where $x_r(0 \text{ deg})$ and $x_r(90 \text{ deg})$ correspond to the backward-facing step and the flat-plate/splitter-plate configurations, respectively. This correlation does not fit the present data well (35% error) partly because the limiting case of $\alpha = 0$ corresponds to $x_r = 0$ in the present configuration. The reattachment length can, however, be approximated within 5% (see Fig. 4) by the following variant of Simpson's correlation:

$$\frac{x_r(\alpha)}{x_r(90 \text{ deg})} = \sin^2\alpha \tag{2}$$

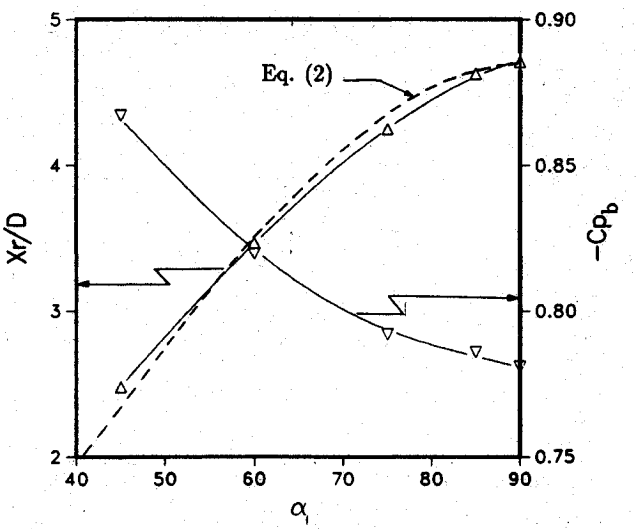

Fig. 4 Variation of reattachment length and base pressure with angle of separation.

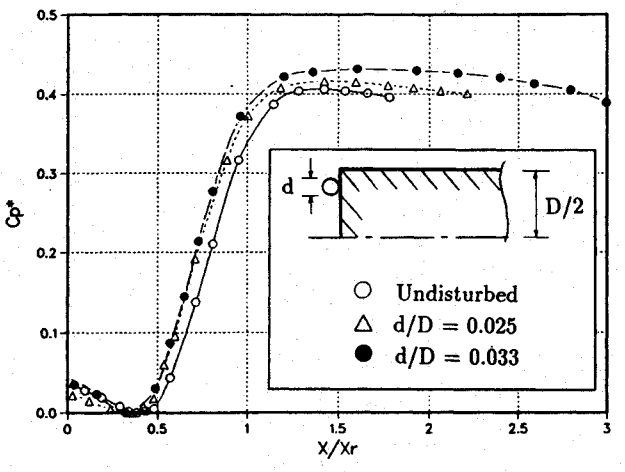

Fig. 5 Effect of tripping the boundary layer on reduced pressure distribution. Data taken from Dziomba.[4]

The trends shown in Fig. 4 are qualitatively similar to the effect of either tripping the boundary layer on the front face before it separates,[4] or increasing the freestream turbulence level.[1,3] Tripping of the boundary layer was reported[4] to reduce the reattachment length by up to 40%, and the base pressure coefficient by 15%. The shortening of the bubble was attributed to an effective change in the separation angle due to the formation of a small recirculation bubble between the trip wires and the sharp leading edge of the plate.

To elucidate this point, the pressure distributions reported in Ref. 4 (measured at UBC using the same base model) were replotted in terms of reduced coordinates for the basic undisturbed flow and two tripped flows using different diameter wires. The results in Fig. 5 show that the collapse, though reasonable, is not as good as that obtained in Fig. 3 with the various leading-edge angles. In particular $C_{P_m^*}$ increases from about 0.4 to 0.43 when the boundary layer is tripped, and the pressure recovery process starts earlier resulting in a shift of the data towards the left. This, together with the proportionally higher decrease in C_{P_b} noticed earlier, indicates that the effect of the trip wire may be partly due to an effective change in the separation angle, but it is not confined to this mechanism. Additional factors to be considered are possible changes in the state of the separating boundary layer and in the initial growth rate of the separated shear layer.

References

[1]Hillier, R., and Cherry, N. J., "The Effect of Stream Turbulence on Separation Bubbles," *Journal of Wind Engineering and Industrial Aerodynamics,* Vol. 8, July 1981, pp. 49-58.

[2]Gartshore, I. S., and Savill, M., "Some Effects of Freestream Turbulence on the Flow Around Bluff Bodies," Euromech 160: Periodic Flow and Wake Phenomena, Berlin, 1982.

[3]Kiya, M., and Sasaki, K., "Freestream Turbulence Effects on a Separation Bubble," *Journal of Wind Engineering and Industrial Aerodynamics,* Vol. 14, 1983, pp. 375-386.

[4]Dziomba, B., "Experimental Investigation of Bluff Body Separation Regions," CASI Aerodynamics Symposium, Montréal, Canada, 1985.

[5]Ota, T., Asano, Y., and Okawa, J., "Reattachment Length and Transition of the Separated Flow Over Blunt Flat Plates," *Bulletin of the Japan Society of Mechanical Engineers,* Vol. 24, June 1981, pp. 941-947.

[6]Djilali, N., and Gartshore, I. S., "Turbulent Flow Around a Bluff Rectangular Plate. Pt. 1: Experimental Investigations," *ASME Journal of Fluids Engineering,* Vol. 113, No. 1, 1991, pp. 51-59.

[7]Castro, I. P. and Dianat, M., "The Pulsed-Wire Skin-Friction Measurement Technique," *Proceedings of the 5th Symposium on Turbulent Shear Flows,* Cornell Univ., Ithaca, NY, 1985, pp. 11.19-11.24.

[8]Roshko, A., and Lau, J. C., "Some Observations on Transition and Reattachment of a Free Shear Layer in Incompressible Flow," *Proceedings of the Heat Transfer and Fluid Mechanics Institute,* edited by A. F. Charwatt, Stanford Univ. Press, Stanford, CA, 1965, pp. 157-167.

[9]Ruderich, R., and Fernholz, H. H., "An Experimental Investigation of a Turbulent Shear Flow with Separation, Reverse Flow, and Reattachment," *Journal of Fluid Mechanics,* Vol. 163, Feb. 1986, pp. 283-322.

[10]Westphal, R. V., Johnston, J. P., and Eaton, J. K., "Experimental Study of Flow Reattachment in a Single-Sided Sudden Expansion," NASA CR-3765, 1984.

[11]Simpson, R. L., "Two-Dimensional Turbulent Separated Flow," AGARDograph 287, 1985.

Prandtl-Meyer Function for Dense Gases

M. S. Cramer* and A. B. Crickenberger†
Virginia Polytechnic Institute and State University, Blacksburg, Virginia 24061

I. Introduction

THE Prandtl-Meyer function plays a central role in the analysis of many steady isentropic flows. The restriction to perfect gases, i.e., those satisfying

$$p = \rho RT \quad \text{with} \quad c_v = \text{const} \tag{1}$$

where p, ρ, R, T, and c_v are the thermodynamic pressure, fluid density, gas constant, absolute temperature, and the specific heat at constant volume, respectively, permits the derivation of explicit formulas for the Prandtl-Meyer function. However, many applications require consideration of dense gas effects. Examples include many industrial and chemical processing systems, power systems, typically those based on the Rankine cycle, and some wind-tunnel designs. The latter take advantage of the large decrease in kinematic viscosity, due both to choice of working fluid and operation at higher pressure, to increase the Reynolds number for a given Mach number.

An important dense gas effect exhibited by many fluids is a decrease in the sound speed during isentropic compression. A nondimensional parameter measuring the variation of sound speed along an isentrope is

$$\tilde{\Gamma} \equiv 1 + \frac{\rho}{a}\frac{\partial a}{\partial \rho}\bigg|_s \tag{2}$$

where

$$a \equiv \left(\frac{\partial p}{\partial \rho}\bigg|_s\right)^{1/2} \tag{3}$$

is the thermodynamic sound speed and s is the fluid entropy. The thermodynamic quantity $\tilde{\Gamma}$ has been termed the fundamental derivative of gasdynamics by Thompson,[1] who demonstrated its significance in virtually all areas of gasdynamics. It is easily verified that

$$\tilde{\Gamma} = \frac{\gamma+1}{2} > 1 \tag{4}$$

Received Aug. 22, 1990; revision received April 5, 1991; accepted for publication April 12 1991.

*Associate Professor, Department of Engineering Science and Mechanics. Member AIAA.

†Graduate Project Assistant, Department of Engineering Science and Mechanics.